JOURNAL OF GEOPHYSICAL RESEARCH

1978

Orbital Radar Evidence for Lunar Subsurface Layering in Maria Serenitatis and Crisium

WAYNE J. PEEPLES,[1] WILLIAM R. SILL, THOMAS W. MAY,[2] AND STANLEY H. WARD

Department of Geology and Geophysics, University of Utah, Salt Lake City, Utah 84112

ROGER J. PHILLIPS, ROLANDO L. JORDAN, ELSA A. ABBOTT, AND TERRY J. KILPACK

Jet Propulsion Laboratory, California Institute of Technology, Pasadena, California 91103

Data from the lunar-orbiting Apollo 17 radar sounding experiment (60-m wavelength) have been examined in both digital and holographic formats. Surface backscatter (clutter) which masks possible radar returns originating from subsurface changes in lunar electrical properties was reduced by simultaneously comparing radar data from two orbits. Radar returns that correlate from orbit to orbit form two distinct alignments in Mare Serenitatis and one in Mare Crisium. It is proposed that these alignments represent subsurface reflecting horizons. The hypothesis is tested by showing that (1) most of the radar returns fall outside the ambiguity region of the correlation technique, (2) the results are consistent between optically and digitally processed data, (3) the signal levels of the proposed subsurface features are well above the noise floor, (4) the inferred loss tangents appear to be consistent with returned sample measurements, and (5) the discontinuous nature of the reflections most likely arises from interference effects. It is concluded that there are two subsurface radar reflectors with mean apparent depths of 0.9 km and 1.6 km below the surface in Mare Serenitatis and one reflector at a mean depth of 1.4 km below the surface in Mare Crisium. These reflectors represent basin-wide subsurface interfaces.

INTRODUCTION

The Apollo lunar sounder experiment (ALSE), a radar experiment included on the Apollo 17 flight, has been described by *Phillips et al.* [1973*a*, *b*]. Further results on lunar altimetry have been reported by *Brown et al.* [1974], while imagining results from the experiment were described by *Maxwell et al.* [1975]. Although these scientific results were important, they were not the prime scientific objective of the ALSE; the experiment was designed to detect and map variations in the subsurface electrical properties and therefore lunar subsurface layering. In this paper we present evidence for basin-wide subsurface layering in Maria Serenitatis and Crisium from the deep-penetrating 5-MHz (HF1) portion fo the lunar sounder experiment. In subsequent papers we will present our geologic interpretation of the mare layering and structure and the implications for basin formation and evolution.

EXPERIMENT DESCRIPTION

The Apollo 17 lunar sounder experiment was a lunar-orbiting, coherent-chirped synthetic aperture radar experiment capable of transmitting radar signals into the lunar subsurface and recording the reflected signals. The HF1 ALSE apparatus consisted of a center-fed dipole antenna, a coherent synthetic aperture radar system, and an optical recorder which recorded the received signal and information about the experimental apparatus. Additional information from the experiment was telemetered to earth during the radar operation. This information included results from a 'specular power monitor' which measured the integrated signal power from radar signals reflected from the moon. The instrumentation is further described by *Phillips et al.* [1973*a*] and *Porcello et al.* [1974].

The experimental equipment and its placement within the spacecraft was designed to minimize possible electromagnetic interference between ALSE equipment and other spacecraft systems and experiments. During the actual data collection in lunar orbit, all nonessential spacecraft systems and other Apollo orbital experiments were not operated as another effort to minimize electromagnetic interference. HF1 ALSE data were continuously collected during Apollo 17 lunar revolutions 16, 17, and 18. Film containing the unprocessed stored data from the optical recorder was returned to earth and developed by using techniques designed to reduce noise and nonlinear development effects.

PROCESSING ALSE DATA

The major difficulty in the determination of lunar subsurface features from the ALSE radar data is the strong off-axis return (clutter) from the lunar surface. The much weaker

subsurface return must be distinguished from this clutter. We have limited our search for subsurface returns to the relatively smooth mare regions in an attempt to reduce the clutter problem.

Surface and subsurface radar returns are separated in time by a few tens of microseconds. Owing to the pulse compression nature of the radar system, individual processed signals have power versus time functions of approximately the form $[\sin(x)/x]^2$, with a large main lobe and side lobes decreasing in amplitude away from the center of the signal. Spectral weighting has been applied to the data to reduce the far range side lobes of the system impulse response to acceptable levels [*Porcello et al.*, 1974]. Although side lobes of the bright quasi-specular surface returns could be mistaken for subsurface returns, in practice these can be identified in the data by their correlation in delay, strength, and Doppler frequency content with respect to the surface return. The range resolution of the HFI system precludes determining subsurface features with time delays of less than about 8 μs (approximately 400 m in depth if we assume a dielectric constant of 8 for the lunar medium) with respect to the HFI surface return.

The ALSE HFI data have been processed by using two different techniques. The returned data were transformed to both holographic and digital formats for subsequent processing, inspection, and interpretation.

The HFI data were originally optically processed for 300-m azimuth (along track) resolution with 50-dB dynamic range and then recorded in a holographic format on film [*Adams et al.*, 1974]. This film was later placed in a specially designed hologram viewer for analysis. The viewer allows the interpreter to adjust Doppler bandwidth and magnify portions of the reconstructed radar image on a viewing screen.

The HFI data were also digitized and stored on magnetic tape for computer processing. A variety of digital processing techniques have been applied to the digital data. These techniques included low-pass filtering and coherent stacking of processed data in the along-track direction by nonoverlapping stacking procedures [*Phillips et al.*, 1973*a*, *b*], and later directional stacking procedures were used in an effort to enhance subsurface returns. The modulation properties of the data in range and azimuth were studied in attempts to define the lunar transfer function. Deconvolution techniques were also applied, but all these techniques met with minimal success.

The Multiple-Orbit Correlation Technique (MOC)

We have concluded from careful inspection that the analysis of radar data collected during a single lunar orbit was not sufficient to obtain an adequate confidence level for subsurface feature detection, chiefly because of the problem of separating subsurface signals from lunar surface derived clutter. Therefore the data were analyzed by using a multiple-orbit data correlation technique to achieve confidence in the determination of subsurface layering. This approach is now described.

The technique involves the geometry of multiple orbits shown in Figure 1. The simplest meaningful assumption regarding a subsurface reflecting layer is a discontinuity in electrical properties located at some uniform depth below the local lunar surface. If this reflector has lateral dimensions as least as large as the orbital separation and the along-track resolution, then the radar return from this subsurface feature will be recorded during each orbit. The radar return from this subsurface reflector will have the same time delay relative to the strong surface reflector for both orbits. Scattering from an individual surface feature will not be recorded at the same relative time delay on both orbits owing to the translation of the orbits.

In detail, in Figure 1 we note that on orbit 1 a subsurface reflector is recorded with time delay

$$t = \frac{2h}{c} + \frac{2\eta(K_1)^{1/2}}{c} \tag{1}$$

where h is the orbital altitude, K_1 is the relative dielectric constant of layer 1, η is the thickness of layer 1, and c is the speed of light in free space. A signal with the same time delay could also be due to an off-track surface reflector S at a distance from the spacecraft ground track

$$X \approx (2h\eta K_1)^{1/2} \tag{2}$$

However, the relative time delay of the subsurface reflector is the same for orbit 2 (assumed to be at the same altitude), while the reflection from S must be delayed (move-out) by

$$\Delta t = \frac{2}{c}\{[h^2 + (\delta - X)^2]^{1/2} - (h^2 + X^2)^{1/2}\} \approx \frac{\delta}{ch}(\delta + 2X) \quad (3)$$

where δ is the ground track separation between the two orbits. Thus reflections with the same relative time delay are more likely to be due to a subsurface layer.

The MOC technique was applied to the holographic imagery in the following manner: A section of the HFT hologram film representing data collected during a spacecraft flyover of a particular lunar area was imaged in the hologram viewer. Photographs of the resulting hologram image were taken and combined into a mosaic at a scale of 1:120,000. Another section of the hologram film representing radar data collected over the same lunar area but obtained from a different orbit was later imaged and photographed. Mosaics of the imagery from each orbit were registered (positioned to a common lunar geographic point) and searched for radar returns which had little or no displacement (move-out) in range from one orbital imagery mosaic to the other mosaic, as shown in Figure 2. The criterion for correlation was that there be at least 80% overlap (in time delay and longitude) between the two signals. This multiple-orbit data correlation procedure was used to search for possible subsurface features in the imagery obtained as the spacecraft passed over the Serenitatis and Crisium basins.

The correlated returns found in the above manner from revolutions (revs) 16 and 18 have been plotted in cross-section form in Plate 1 for Mare Serenitatis. A similar plot from revs 17 and 18 for Mare Crisium is shown in Plate 2. Time delay relative to the nadir surface return has been converted to distance by assuming that the lunar material has a relative dielectric constant of 8.7. We note that amidst a background of random reflections, there are two sets of aligned reflections in Serenitatis and a single aligned reflection in Crisium. The coherent alignments of images do not appear as a continuous linear image but take the form of a discontinuous set of radar returns. The returns are of short duration (300–1000 m in azimuth) and are separated by distances ranging from 300 m to a few kilometers in Serenitatis and up to a few tens of kilometers in Crisium.

We will refer to the aligned correlated reflections as 'events,' and we hypothesize that these events are subsurface reflections. The hypothesis will be tested by the following questions: (1) What are the interpretational ambiguities in the MOC technique? (2) Do these events appear in both digital and holographic data formats? (3) Can we identify surface returns in the data? (4) Are the proposed subsurface events well above the data noise level? (5) Are the strengths of the returns consistent with the known dielectric and loss tangent properties of returned lunar samples? (6) Why are the events composed of discontinuous reflections?

MOC Interpretational Ambiguity

If we could experimentally measure time delay with negligible error, surface reflectors and subsurface features would be distinguishable unless a surface reflector lay midway between orbital tracks or two surface reflectors were each situated the same distance from both ground tracks. In practice, the time delay of a reflector's signal has an associated error, which we experimentally estimate to be 1.2 μs. Hence we cannot measure the move-out (Δt) of a signal between two orbits if it is less than 2 μs.

To define the region of ambiguity between surface and subsurface reflections, we invert (3) for X and set Δt to a value of 2 μs. For two orbits of known orbital track separation δ a band of ambiguity on the lunar surface can be determined. The band of ambiguity simply defines that region on the surface where a surface scatterer will show less than 2 μs of move-out between orbits and thus cannot be distinguished from a zero-move-out subsurface reflector.

The boundary of such a band is plotted in Figure 3 as the 2-μs move-out distance X for Mare Serenitatis, using revs 16 and 18. The band of ambiguity extends X km north of the northerly orbit and a similar distance south of the southerly orbit. The separation distances for the two orbits range from 0 km near 28°E longitude to 4.3 km at 12°E longitude. The corre-

lated reflections for Mare Serenitatis are also plotted in Figure 3b by assuming that they arise from the surface and converting time delay to equivalent distance from the nadir (ground track) position. By our arguments, however, it is not possible for a single surface reflector to lie above the 2-μs curve. We tend to reject then, at least for western Serenitatis, the idea that the correlated reflections could arise from a single surface feature.

For Mare Crisium the orbital ground track separation is a constant 5 km (Figure 4). The event detected in Mare Crisium lies well above the 2-μs line.

It could be argued that correlation is due to two surface reflectors at different locations with an identical time delay on each orbit. While this is certainly a possibility, it is difficult to generate anything other than a random pattern in the cross sections. A random distribution of scatterers with a preferred slope, however, could produce correlated returns in an organized pattern. For each orbit, strong returns would arise for those scatterers at a distance where the preferred slopes presented a specular facet to the radar. The distance, and hence time delay, would be independent of orbit and thus would give rise to correlated features. The obvious candidate for random scatterers would be craters. It seems unreasonable that craters in Crisium would have one preferred slope while craters in Serenitatis would have two preferred slopes. For such a scattering mechanism, however, changes in the time delay of the events with longitude would imply a change in crater morphology, age, or target composition, and/or a change in the regional slope on which the craters are superimposed. As an example, consider the change in depth (or time delay) of the lower event in Serenitatis (Plate 1), from 22.2° to 22.7°E. For a surface interpretation the preferred slope must change from 1.5° to 4.4° in about 14 km. This region appears to be in a single basalt unit [*Howard et al.*, 1973] of a constant age [*Boyce and Dial*, 1973], and the total regional change in topography is less than 50 m (lunar topographic orthophoto map42C4). We conclude that this surface mechanism for producing correlated features is highly unlikely.

Analysis of Data in a Digital Format

Figure 5*a* shows a contoured representation of the optically azimuth focused, digitally range compressed HF1 data for the region near the crater Descilligny in Mare Serenitatis. The data were taken during rev 18, and we have applied the MOC technique to this digital image paired with the equivalent image for rev 16. The correlated reflections are shown in black. A heavy line is drawn through the nadir specular reflection, and the time reference is set to 0 μs at this point. Two additional lines are drawn through apparent alignments of correlated events, and we hypothesize that these two alignments represent subsurface reflectors.

There are two dominant surface features in the vicinity of the ground tracks, the crater Descilligny and Dorsa Lister, a wrinkle ridge. The dashed ellipses centered on the 40-μs range delay indicate the calculated time delays of the radar returns from the rim and floor perimeters of Descilligny. There is a strong return (−15 dB with respect to the surface specular flash) associated with the north interior wall of this crater. Data from rev 16 show a return from the floor with an increase in range time delay of 5 μs. This is the appropriate move-out for the shift of the ground track between revs 16 and 18. The ground track of rev 18 is about 1.5 km north of the rev 16 ground track, a position placing it closer to the crater Descilligny.

The sloping dashed line in Figure 5*a* shows the radar reflections from Dorsa Lister projected into the cross section. It is clear that Dorsa Lister accounts for some of the shaded coherent events, since the reflected energy from the ridge should show a 2-μs movement between rev 16 and rev 18 data. As we discussed above (see Figure 3), this is at the limit of our time delay measurement accuracy. Larger movement, as in the case of crater Descilligny, is more readily measured.

Since we have been able to make positive identification of known surface features in the data, we argue that alignments in the cross sections which do not correlate with observable surface features are more likely to arise from subsurface reflections. Indeed, we find very little correlation between the correlated events in Plates 1 and 2 and surface features.

Since the holographic and digital data arise from different data-processing schemes, it is useful to compare alignments from both data sets as a self-consistency check. The two dominant events found in the hologram studies have been shown as solid lines on Figure 5*b*, and these correlate well within the positioning errors of the digital events.

Signal-to-Noise Ratio

An important test of the subsurface hypothesis is that the events shown in Plates 1 and 2 are situated well above the data noise level. There are four important sources of noise: (1) film noise, (2) spacecraft noise, (3) cosmic noise, and (4) earth noise.

The film dynamic range is 30 dB [*Porcello et al.*, 1974], and signal compression of the chirped radar pulse adds an additional gain of 17 dB. This yields a signal-to-film noise ratio of 40 dB or greater, depending on the proximity of the strong nadir specular surface returns to the exposure saturation level of the data-recording film. The hypothesized subsurface events are typically no weaker than 25 dB below the nadir returns, and we thus discount film noise as an important noise source.

The ALSE HF receivers (5 and 15 MHz) had a capability to measure the noise background directly and telemeter this information directly to earth, bypassing the film recording. On the lunar farside the noise brightness measurement compared favorably with the cosmic noise measurements of earlier workers [*Phillips et al.*, 1973*a*]. We can thus conclude that the spacecraft noise level lies below the cosmic noise level.

The dominant noise contribution is, in fact, earth noise [*Phillips et al.*, 1973*b*], which is about 15 dB stronger than cosmic noise [*Killpack*, 1975]. The noise intensity shows a distinct correlation with local time at the sublunar point on the earth, being a maximum at earth nighttime.

The noise measurements were absolutely calibrated in terms of the characteristics of the antenna and receiver. We do not know the actual earth noise level at the time of the sounding but must rely on ALSE receiver 'noise only' measurements taken during other parts of the radar experiment and our understanding of the noise variation with local earth time. In the digitally processed data we estimate the near-earth noise level at −106 ± 3 dBW (decibels below 1 W). The digitally processed signal is not absolutely calibrated per se, but this process may be accomplished by tying the signal level to the calibrated specular power monitor output data taken during the same time, taking due account of bandwidths of the equipment and pulse compression characteristics.

In Figure 6 we present an amplitude versus time trace taken at the location indicated by the vertical dotted lines on Figure 5. As estimated from the specular power monitor, the nadir specular return has a level of −65 dBW. Our estimate of the earth noise is shown in the shaded region. To the left of the nadir specular reflection are only the decreasing side lobes preceding the main lobe of this reflection and earth noise. The signal level does indeed drop down to our estimated earth noise level. Also shown are a near-nadir surface reflection, the hypothesized subsurface reflections, and the general background of surface clutter. By inspection of Figure 6 it is seen that we are dealing with adequate signal margins in our hypothesized subsurface events.

Inferred Electrical Properties

The electromagnetic plane wave power reflection coefficient at a plane interface between two dielectric media depends on the ratio of the dielectric constants as

$$r_{12} = \left| \frac{1 - (K_2/K_1)^{1/2}}{1 + (K_2/K_1)^{1/2}} \right|^2 \tag{4}$$

where K_i is the relative dielectric constant of the ith medium.

In the mare regions, most surfaces are probably regolith covered; however, at depths of the order of a few to tens of meters, solid-rock interfaces should be encountered. Again if a plane wave–plane layer interface is assumed, the apparent surface reflection coefficient for this type of interface is [*Stratton*, 1941, p. 514]

$$R = \frac{(r_{12} + r_{23})^2 - 4r_{12}r_{23}\sin^2(2\pi d/\lambda)}{(1 + r_{12}r_{23})^2 - 4r_{12}r_{23}\sin^2(2\pi d/\lambda)} \tag{5}$$

where d and λ are the thickness of and the wavelength in layer 2, respectively.

With the dielectric constant increasing from medium 1 (free space) to medium 2 (regolith) to medium 3 (rock), the reflection coefficient has minima for d at odd multiples of quarter wavelengths and maxima for d at even multiples of quarter wavelengths. For dielectric constants of 3 for the soil and 6 for the rock these maximum and minimum reflection coefficient values are approximately 0.17 and 0.01. Variations in the reflected specular power do show variations, but we cannot unambiguously state whether these variations are due to regolith depth changes, interference from surface clutter, or changes in electrical properties.

The plane wave reflection coefficient from a buried rock-rock interface is determined by (4). Thus a rock-rock interface separating materials with dielectric constants of 7 and 9 has a power reflection coefficient of 4×10^{-3}. A deep-lying density inversion may provide another type of interface. In this case a medium of lower dielectric constant (presumably, a buried regolith or pyroclastic layer) is surrounded by rock of higher dielectric constant (presumably basalt). The reflection coefficient can be several times larger than that expected for a rock-regolith interface and considerably larger than that expected for the rock-rock type of interface.

The power ratio between the subsurface and the surface signals expressed in decibels is

$$\Delta(\mathrm{dB}) = 10 \log [(1 - r_{12})^2 / r_{12}] + 10 \log r_{23} - 27.3 f \tau \tan \delta \qquad (7)$$

where

- r_{12} power reflection coefficient of the free space–lunar surface interface;
- r_{23} power reflection coefficient of the buried reflector;
- $\tan \delta$ loss tangent of material between the surface and the buried interface;
- f frequency;
- τ time delay of subsurface echo.

The most favorable conditions for detecting subsurface radar returns occur when the surface reflectivity is low and the subsurface echo is from a buried density inversion with a thickness near one-quarter wavelength.

Typical echo strengths for the hypothesized subsurface events generally range from −20 dB to −30 dB with respect to the surface return. The loss tangents calculated from (7) with these values and an assumed depth of 1600 m yield a typical upper bound of 1×10^{-2}, the larger values being calculated from a buried density inversion. The upper bound is calculated for a surface regolith thickness of about 7 m and a buried density inversion thickness of about 5 m. Decreasing the density inversion thickness to 2 m lowers the upper bound on loss tangent to 8×10^{-3}. The worst combination of the two thicknesses yields an upper bound of about 4×10^{-3}.

It is not possible to relate these values of loss tangent to returned sample measurements because there are no samples of central Serenitatis mare material. There are also few measurements of returned samples at 5 MHz. Further, although there has been significant reduction in the levels of introduced water in measured samples, it is not possible to demonstrate the complete absence of residual contamination.

We believe, however, that the range of calculated loss tangents from 4×10^{-3} to 1×10^{-2} is consistent with the laboratory measurements [*Olhoeft and Strangway*, 1975]. Further, the mascon mare exhibit low TiO_2 content [*Johnson et al.*, 1977], and there is a definite positive correlation between TiO_2 content and loss tangent.

At the same time it is likely that a buried density inversion is required to explain the results. By using the extreme range of 7–9 for reported basalt dielectric constants [*Olhoeft and Strangway*, 1975] and the most favorable surface regolith thickness the maximum loss tangent calculated is 6×10^{-3}.

The Discontinuous Nature of the Radar Reflections

Several effects could cause the hypothesized subsurface features to appear as a discontinuous series of aligned correlated features. We postulate two possibilities:

1. The subsurface feature is actually discontinuous in nature and only occasionally presents subsurface facets properly oriented to reflect enough energy to be detected experimentally.

2. The subsurface is continuous, but other phenomena produce a discontinuous effect in our data (e.g., constructive and destructive interference between the subsurface radar return and surface clutter returns). To examine our first hypothesis, we modeled a properly oriented subsurface facet as a circular aperture in a perfectly conducting plane and calculated the effects of Fraunhofer diffraction [*Jackson*, 1963, pp. 292–297] for a normally incident plane wave. Results of this calculation indicate that the observed signal returns cannot be physically generated by circular facets of the order of 500 m in diameter because an additional signal weakening of at least −20 dB would be introduced. This in turn would lead to unreasonably low loss tangent values. We therefore believe that our first hypothesis is refuted.

The second hypothesis, that the subsurface layers are in fact continuous, is the hypothesis that we accept. An examination of the original data shows that interference effects are present among the scattered surface signals, and it seems also likely that the discontinuous nature of the hypothesized subsurface events is also caused primarily by interference effects. We conclude that the events in Serenitatis and Crisium (Plates 1 and 2) are produced by basin-wide disconformities in the subsurface electrical properties.

Summary

We have presented the following evidence that many of the spatially coherent events detected in Mare Serenitatis and Mare Crisium arise from subsurface reflectors.

1. Common radar returns align in an approximately horizontal fashion which indicates that the reflections arise from either subsurface reflectors or linear surface features that are aligned approximately parallel to the ground tracks.

2. If there is ample ground track separation, then a move-out criterion can be applied to separate the above possibilities. There is enough separation between ground tracks in Mare Crisium and most of Mare Serenitatis to indicate strongly that the alignment does not arise from linear surface features.

3. Surface features such as craters and wrinkle ridges are recognizable in the data. We use this result to argue the converse: When the coherent events do not correlate with surface features, we consider this as evidence that these alignments arise from subsurface reflectors.

4. The proposed subsurface events are self-consistent between optically and digitally processed data.

5. The signals associated with the proposed subsurface features are well above the data noise level.

6. The fact that the coherent events persist over a large portion of the basin diameter lends credence to the subsurface nature of these reflections and makes it less likely that the alignments arise from surface features.

7. The strength of the deepest alignment indicates lunar loss tangents ranging from 4×10^{-3} to 10^{-2}, consistent with measurements on returned lunar samples. The reflections most likely arise from density inversions, presumably a buried regolith or pyroclastic layer.

8. The along-track variations of the alignments correlate in a geologically meaningful way with structural and compositional features on the surface. As an example, the surface projection of the dipping boundaries of the shallowest reflector in Serenitatis appears to coincide with the contact between the dark annulus mare unit and the lighter mare of the central part of the basin. Further, by linearly extending the topographic slope of the dark annulus material in southern Serenitatis northward into the basin, the calculated depth at the Apollo 17 ground tracks is within 50 m of the depth of the shallow reflector. We thus interpret the shallow reflector as the basin-wide contact between the dark annulus unit and the central basalt unit. Detailed stratigraphic and structural interpretations will be the subject of future papers.

On the basis of the above arguments we conclude that the two radar reflectors in Serenitatis and the one reflector in Crisium arise from subsurface layering.

We also point out that radar depth sounding of the terres-

trial bodies of the solar system would seem to be possible under the four conditions of (1) low loss tangent, (2) surfaces no rougher than the lunar mare, (3) ground track separation appropriate to use the move-out criterion, and (4) the availability of high-quality surface imaging as support data.

Acknowledgments. The authors acknowledge the assistance of Ted Maxwell and Johnson Spacecraft Center personnel during the definition, collection, and reduction of the ALSE data. We particularly wish to acknowledge the help of Walter E. Brown, Jr., and Floyd Roberson. We appreciate the critical comments of G. Schaber and two anonymous referees. This research was supported by National Aeronautics and Space Administration contracts NAS 9-12168 and NSG 7090 at the University of Utah and NAS 7-100 at the Jet Propulsion Laboratory, California Institute of Technology.

References

Adams, G. F., P. L. Jackson, J. S. Zelenka, L. J. Porcello, W. D. Hall, F. B. Champagne, and W. G. Carrara, Image and holographic processing, digitization and special investigations of Apollo lunar sounder data, *Tech. Rep. 191500-49-F*, Radar and Opt. Div., Environ. Res. Inst. of Mich., Ann Arbor, 1974.

Boyce J. M., and A. L. Dial, Jr., Stratigraphic studies, C, Relative ages of some near-side mare units based on Apollo 17 metric photographs, *NASA Spec. Publ., 330*, 29-26–29-28, 1973.

Brown, W. E., Jr., G. F. Adams, R. E. Eggleton, P. Jackson, R. Jordan, M. Kobrick, W. J. Peeples, R. J. Phillips, L. J. Porcello, G. Schaber, W. R. Sill, T. W. Thompson, S. H. Ward, and J. S. Zelenka, Elevation profiles of the moon, *Geochim. Cosmochim. Acta, 3, Suppl. 5*, 3037–3048, 1974.

Howard, K. A., M. H. Carr, and W. R. Muehlberger, Stratigraphic studies, A, Basalt stratigraphy of southern Mare Serenitatis, *NASA Spec. Publ., 330*, 29-1–29-12, 1973.

Jackson, J. D., *Classical Electrodynamics*, John Wiley, New York, 1962.

Johnson, T. V., R. S. Saunders, D. L. Matson, and J. A. Mosher, A TiO_2 abundance map for the northern maria, *Geochim. Cosmochim. Acta, A, Suppl. 8*, in press, 1977.

Killpack, T. J., Apollo 17 specular power monitor data—passive mode, M.S. thesis, Dep. of Geol. and Geophys., Univ. of Utah, Salt Lake City, 1975.

Maxwell, T. A., F. El-Baz, and S. H. Ward, Distribution, morphology and origin of ridges and arches in Mare Serenitatis, *Geol. Soc. Amer. Bull., 86*, 1273–1278, 1975.

Olhoeft, G. R., and D. W. Strangway, Dielectric properties of the first 100 meters of the moon, *Earth Planet. Sci. Lett., 24*, 394–404, 1975.

Phillips, R. J., G. F. Adams, W. E. Brown, Jr., R. E. Eggleton, P. Jackson, R. Jordan, W. I. Linlor, W. J. Peeples, L. J. Porcello, J. Ryu, G. Schaber, W. R. Sill, T. W. Thompson, S. H. Ward, and J. S. Zelenka, Apollo lunar sounder experiment, *NASA Spec. Publ., 330*, 22-1–22-26, 1973*a*.

Phillips, R. J., G. F. Adams, W. E. Brown, Jr., R. E. Eggleton, P. Jackson, R. Jordan, W. J. Peeples, L. J. Porcello, J. Ryu, G. Schaber, W. R. Sill, T. W. Thompson, S. H. Ward, and J. S. Zelenka, The Apollo 17 lunar sounder, *Geochim. Cosmochim. Acta, 3, Suppl. 4*, 2821–2831, 1973*b*.

Porcello, L. J., R. L. Jordan, J. S. Zelenka, G. Adams, R. J. Phillips, W. E. Brown, Jr., S. H. Ward, and P. L. Jackson, The Apollo lunar sounder radar system, *Proc. IEEE, 62*(6), 769–783, 1974.

Stratton, J. A., *Electromagnetic Theory*, McGraw-Hill, New York, 1941.

(Received February 4, 1976;
revised January 28, 1978;
accepted February 27, 1978.)

Paper number 8B0208.
0148-0227/78/0068B-0208$03.00

Fig. 1. The geometry of the multiple-orbit correlation technique. The spacecraft is denoted for two orbits (spacecraft orbit perpendicular to plane of figure) at height h and orbital separation δ. A subsurface reflecting layer is at depth η, and a surface reflector S is at an off-track distance X from the nadir point of orbit 1.

Fig. 2. The general scheme for detection of subsurface features using the holographic data. The holographic images of ALSE data for two different orbits are first photographed. The photographs are then registered, and the lunar coordinates are determined from experiment and ephemeris information and searched for correlations of radar returns. All correlations are then plotted as indicated in the lower diagram.

Plate 1. A photomosaic of Apollo 17 metric camera frames AS17-0449, -0452, -0803, and -0806 showing the Apollo 17 ground track for revolution 16 in Mare Serenitatis. Below drawn to the same horizontal scale are shown the coherent ALSE radar returns. The exaggerated vertical scale is in kilometers above the mean radius of 1730 km.

Plate 2. A photomosaic of Apollo 17 metric camera frames AS17-0422, -0424, -0426, -0428, -0430, and -0432 showing the Apollo 17 ground track on Mare Crisium for revolution 18. Below drawn to the same horizontal scale are shown the coherent ALSE radar returns. The exaggerated vertical scale for radar returns is in kilometers above the mean radius of 1730 km.

Fig. 3. The locus of points in Mare Serenitatis for which surface features at a distance X outward from either ground track will move out 2 μs in time delay between revs 16 and 18. Also shown are the placements of the two coherent events, assuming that they arise from surface features.

Fig. 4. The locus of points in Mare Crisium for which surface features at a distance X outward from either ground track will move out 2 μs in time delay between revs 17 and 18. Also shown is the placement of the coherent event, assuming that it arises from a surface feature.

Fig. 5. (*a*) A contoured version of the digitally processed ALSE data. The contours enclose the regions of radar returns that are less than −15 dB, between −15 and −20 dB, and −20 to −25 dB down from the surface specular return. Small closed contours with a bar indicate energy in the −15- to −20-dB range, and small closed contours with no bar indicate the 20- to −25-dB range. The events in black are those which correlated on revs 16 and 18. The dashed ellipses indicate calculated radar returns from crater Descilligny, and the sloping dashed line is the calculated return from Dorsa Lister. The upper solid line represents the surface radar return, and the other two solid lines are a linear interpolation through the coherent events. The vertical dotted line indicates the position of the power versus time trace of Figure 6. (*b*) The same contoured digital data as in Figure 5*a*, where the upper line represents the surface radar return and the lower solid lines indicate coherent radar returns determined from hologram imagery.

Fig. 6. A power versus time trace of the digital data taken at the position shown on Figure 5. Time is arbitrarily referenced to zero at the nadir specular reflection. The power is in dBW, decibels referenced to 1 W. The shaded area indicates the estimate of the earth noise level.

[1] Now at Department of Geological Sciences, Southern Methodist University, Dallas, Texas 75275.
[2] Now at Engineering Geoscience Group, University of California, Berkeley, California 94720.

E.O.T. Counter 0000 Errors 00 Last 000

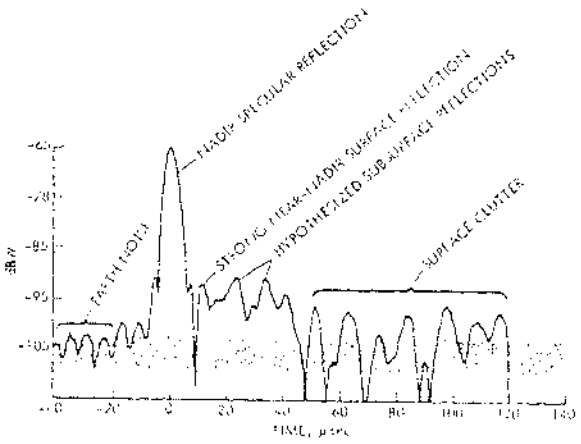

AGU B0208

Au. Peeples et al.

Return to Au ☐

Other Instructions

Fig. 6

50%

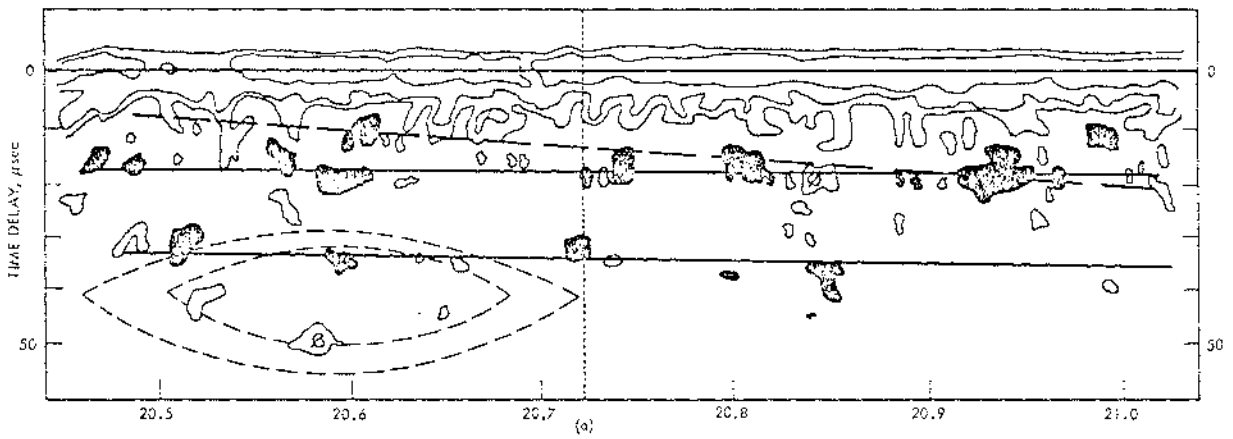

AGU B0208

Au. Peeples et al.

Return to Au ☐

Other Instructions

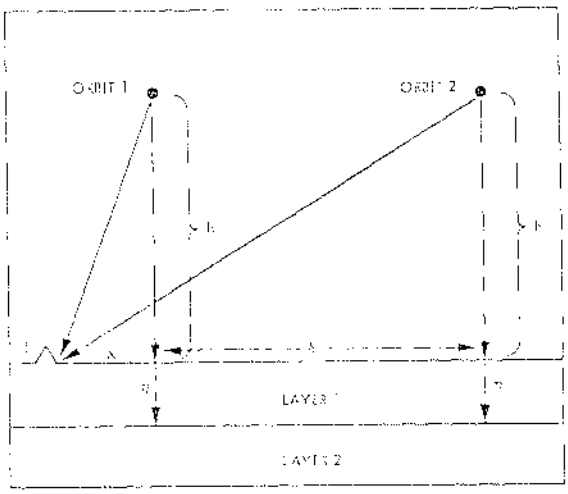

AGU 80208

Au Peeples at al.

FIG. 1

SIZE 50%

Return to Au ☐

Other Instructions

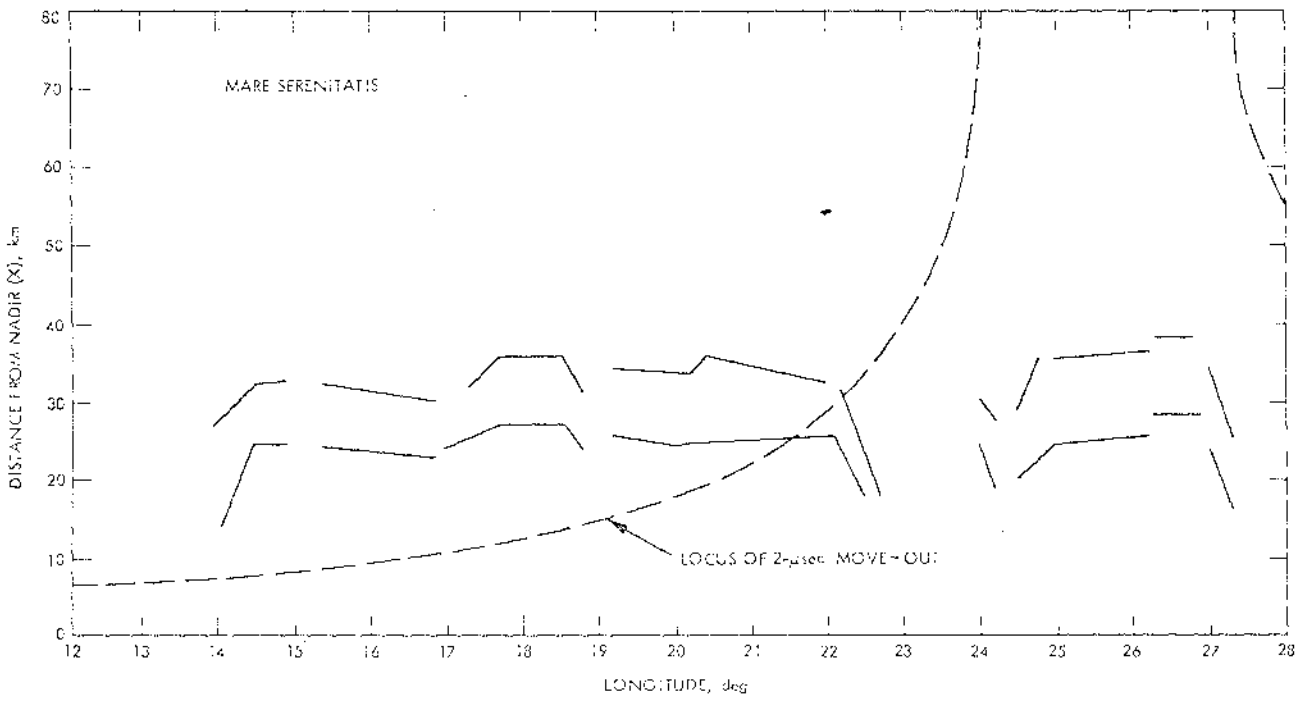

AGU 80208

Au Peeples at al.

FIG. 3

SIZE

Return to Au ☐

Other Instructions

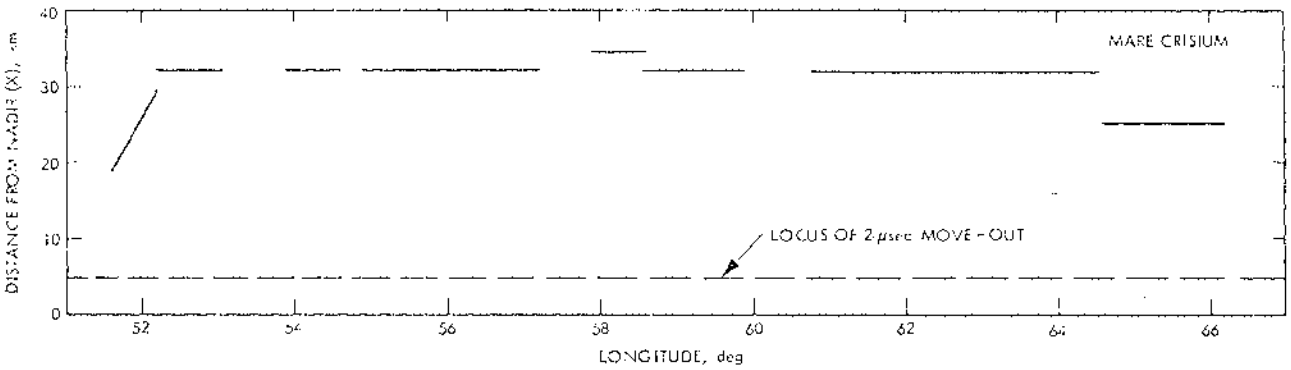

AGU 80208

Au Peeples et al.

Fig 4

SIZE

75%

Return to Au ☐

Other Instructions

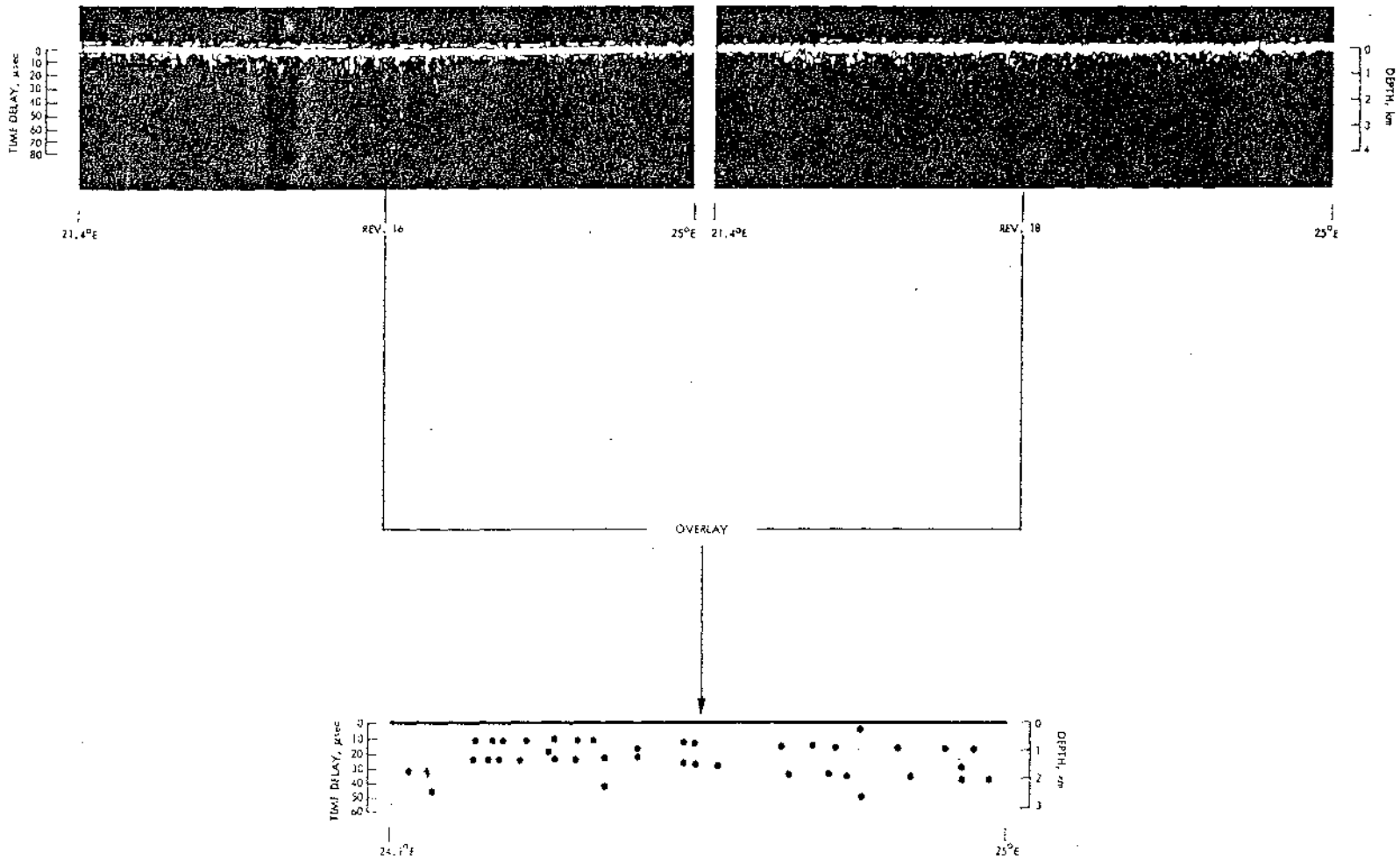

AGU B02208

Au. Peeples et al.

Fig. 2

SIZE

Return to Au ☐

Other Instructions

11

PLATE I PEEPLES

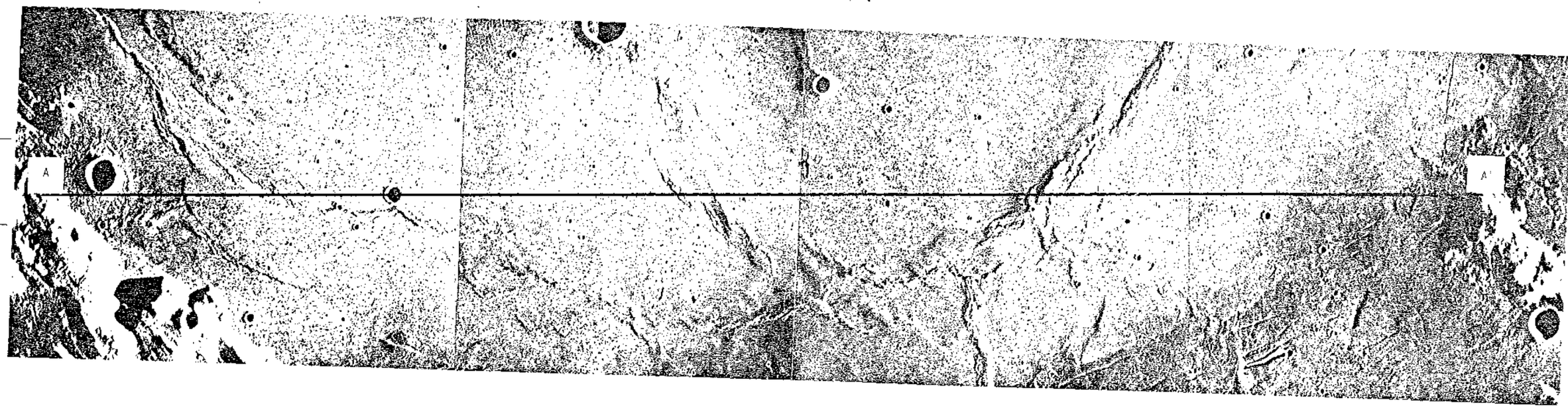

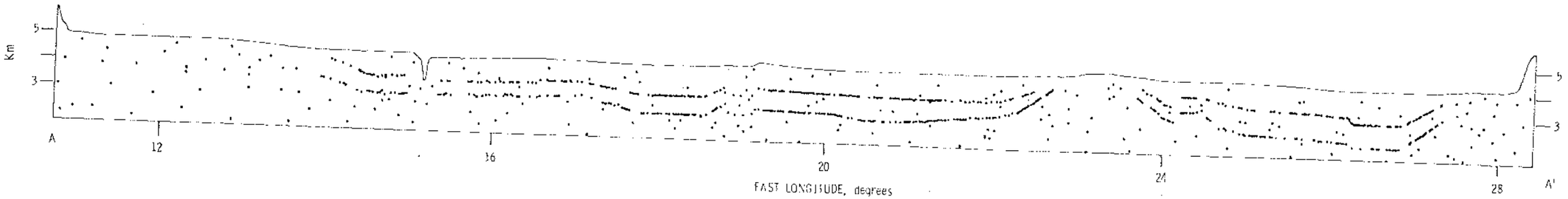

SCALE: 0 50 Km

PEEPLES PLATE 2

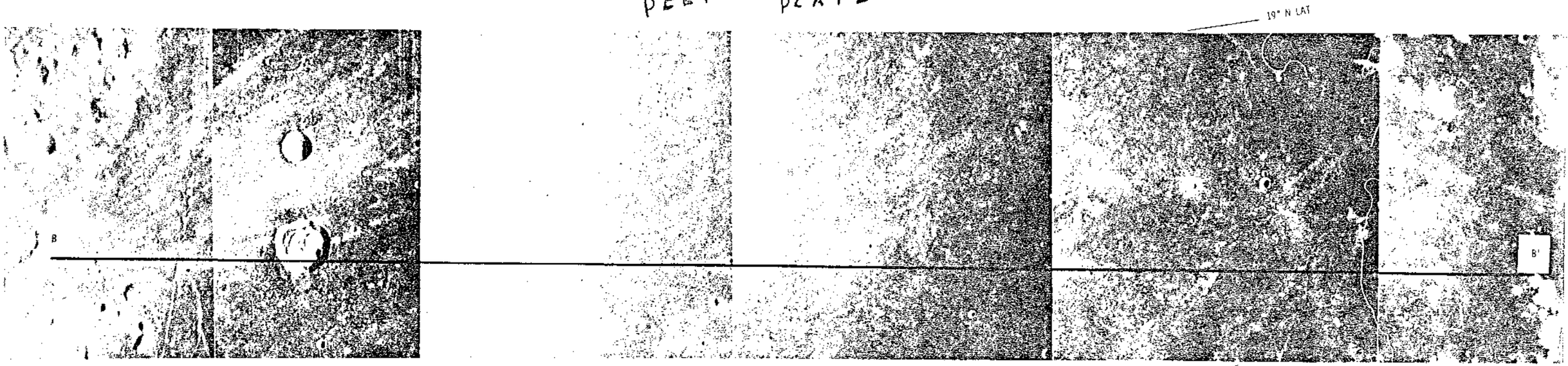

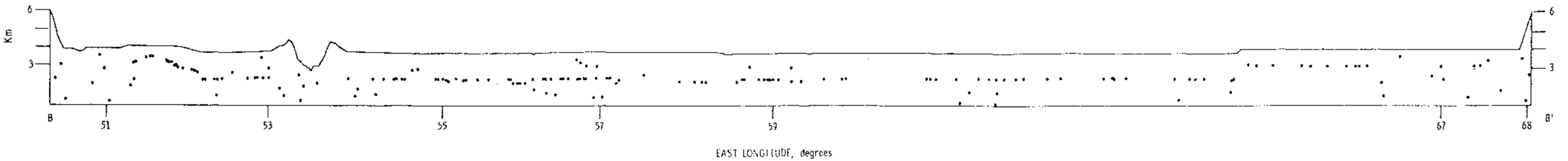

SCALE: 0 50 Km

PEEPLES PLATE 2

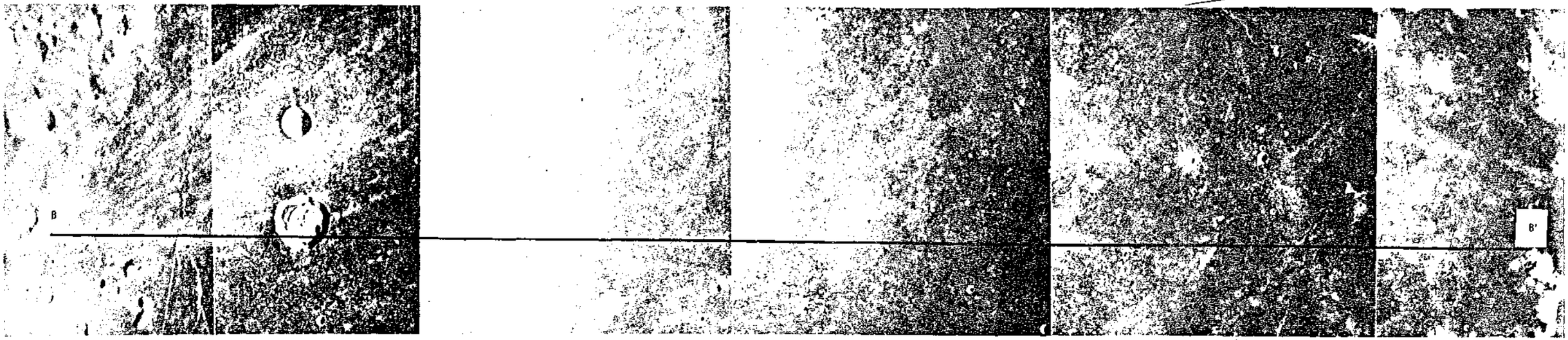

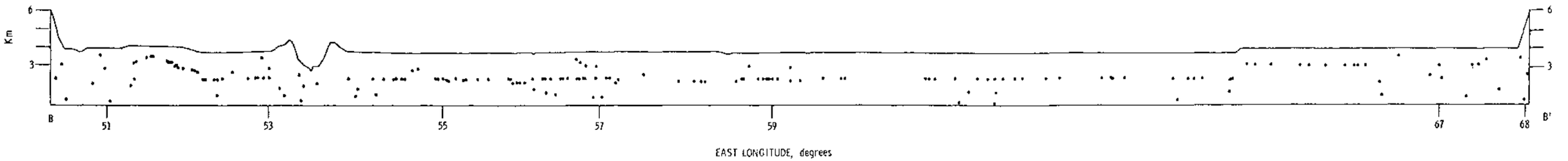

EAST LONGITUDE, degrees

SCALE: 0 50 Km